The Resistive Wall Mode and Feedback Control Physics Design in NSTX*

S.A. Sabbagh 1), J. Bialek 1), R.E. Bell 2), A.H. Glasser 3), B. LeBlanc 2), J.E. Menard 2), F. Paoletti 1), M.G. Bell 2), R. Fitzpatrick 4), E. Fredrickson 2), A.M. Garofalo 1), D. Gates 2), S.M. Kaye 2), L.L. Lao 5), R. Maingi 6), D. Mueller 2), G.A. Navratil 1), D. Stutman 7), W. Zhu 1), and the NSTX Research Team

1) Department of Applied Physics and Applied Mathematics, Columbia University, New York, NY, USA
2) Princeton Plasma Physics Laboratory, Princeton University, Princeton, NJ, USA
3) Los Alamos National Laboratory, Los Alamos, NM, USA
4) University of Texas at Austin, Austin, TX, USA
5) General Atomics, San Diego, CA, USA
6) Oak Ridge National Laboratory, Oak Ridge, TN, USA
7) Johns Hopkins University, Baltimore, MD, USA

e-mail contact of main author: sabbagh@pppl.gov

Abstract. The National Spherical Torus Experiment, NSTX, has been designed to investigate the physics of ST global mode stabilization. NSTX has R_0 = 0.86 m, a midplane half-width of 0.7m, on-axis vacuum toroidal field, $B_0 \leq 0.6$ T, and has reached I_p = 1.5 MA. Experiments have established the wall-stabilized MHD operating space of the device. Maximum β_t and β_N have reached 35% and 6.5, respectively, with β_N reaching 9.5 l_i. Collapses in plasma toroidal rotation and β_t have been correlated to violation of the n = 1 ideal MHD beta limit computed by the DCON stability code using time-evolving EFIT reconstructions of experimental discharges. The resistive wall mode (RWM) was observed over a wide range of β_N. Plasma toroidal rotation damping during the RWM was sudden and global. Damping rates were six times larger than that caused by low toroidal mode number rotating modes, which displayed a slower, diffusive rotation damping away from the rational surface. Rotation damping rate and dynamics depends on the computed minimum value of the safety factor. The computed RWM perturbed field structure from experimental plasma reconstructions has been input to the VALEN feedback analysis code for quantitative comparison of experimental and theoretical mode growth rates, and to analyze the effectiveness of various active feedback stabilization designs. The computed RWM n = 1 mode growth rate, which depends on plasma equilibrium parameters such as β_N and pressure profile peaking, agrees well with experimental growth rates in different operating regimes. Increasing β_N in the ST initially improves mode coupling to the stabilizing wall, however at the highest β_N values reached, mode migration toward the divertor region reduces passive stabilizer effectiveness. Several active mode control designs were considered. The most effective configuration is computed to provide stabilization at β_N up to 94% of the ideal with-wall limit.

1. Introduction

Efficient fusion reactor designs maximize the ratio of the confined plasma energy to the applied magnetic field. The low aspect ratio spherical torus (ST) design utilizes favorable magnetic field geometry to improve plasma stability at reduced toroidal field. Further increases in $\beta_t \equiv 2\mu_0 \langle p \rangle / B_0^2$ and $\beta_N \equiv 10^8 \langle \beta_t \rangle a B_0 / I_p$ can be had by equilibrium profile optimization and passive / active control of global instabilities. Active mode control is expected to be important for fusion reactors since plasmas in these devices may not have sufficient rotation speed to rely upon passive stabilization alone. MHD stability limits, resistive wall mode (RWM) characteristics, mode to conducting wall coupling, and instability growth rates are significantly altered in ST magnetic field geometry compared to moderate aspect ratio devices. Experimental verification and theoretical understanding of these physics elements in the ST are required for a practical design of a global instability control system. Of particular importance in scaling present experimental results to larger devices is understanding the physical mechanisms that most severely increase plasma toroidal rotation damping in the ST.

2. Wall-stabilized Operating Space

The National Spherical Torus Experiment, NSTX, was designed to investigate the physics of global MHD mode stabilization at low aspect ratio. The device has a major radius, $R_0 = 0.86$ m, midplane half-width of 0.7 m, and on-axis vacuum toroidal field, $B_0 \leq 0.6$ T, and has operated at a plasma current, I_p = 1.5 MA. High beta operation with equilibria reaching the ideal "no-wall" MHD stability limit, $\beta_{Nno\text{-}wall}$, (β_t = 25%, β_N = 4.3) was previously reported and a path toward wall-stabilized, high beta operation was described (see Fig. 14 of Ref. [1]). Limitation of β_N to the ideal no-wall limit (at a maximum of $6l_i$) indicated that the passive stabilizer plates in the device had minimal effect on gross plasma instabilities. However, in recent experiments, plasmas have significantly exceeded the ideal no-wall limit, and have reached $\beta_N/\beta_{N\ no\text{-}wall}$ = 1.35. The present wall-stabilized operating space is shown in FIG. 1. Present maximum beta values are β_t = 35%, and β_N = 6.5. The poloidal beta, β_p, has exceeded unity. The ratio β_N/l_i has reached 9.5, and wall stabilization has eliminated the constraint expected by advanced tokamak empirical beta limit scalings in which β_N/l_i is constant [2]. However, the previous trend of maximum β_N increasing with decreasing pressure profile peakedness, F_p, remains true for wall-stabilized plasmas (FIG. 2). Global plasma parameters are reconstructed with the EFIT code [3] using partial kinetic pressure profile information and the measured plasma diamagnetism [1].

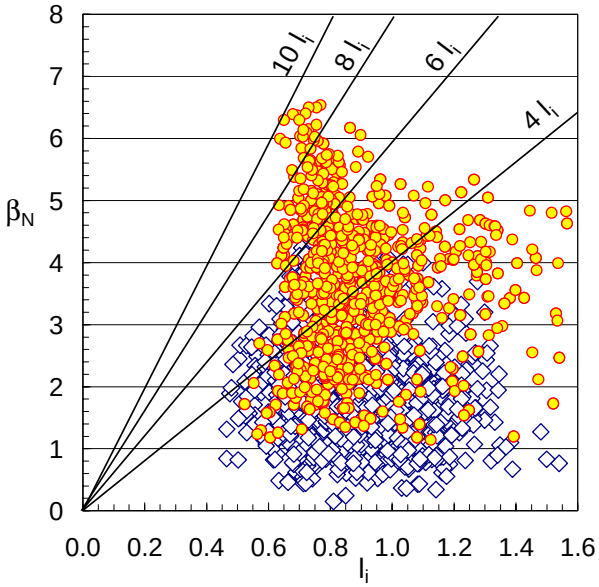

FIG. 1. Normalized beta vs. plasma internal inductance. Recent NSTX plasmas (shaded circles) have exceeded the CY01 nominal "no-wall" beta limit of 6 li.

Recent expansion to increased β_N is related to three key operational and device improvements. First, routine H-mode operation [4] has created plasmas with pressure peaking factors below 1.9. Ideal MHD stability calculations show that broader pressure profiles yield global modes that are more external and therefore amenable to stabilization by the passive stabilizer plates. Second, the static error field in the machine has been significantly reduced by realignment of a main shaping field coil. This improvement has reduced the n=1 static error field by greater than an order of magnitude [5]. This is expected to reduce the negative impact of tearing and resistive wall modes on plama performance and longevity. Finally, both magnetics-only and partial kinetic EFIT reconstructions indicate that the minimum q value, q_{min}, in long pulse, high β_N plasmas is maintained above unity and increases in time to values greater than 2. This is initially due to an increase in the vacuum field to $B_0 > 0.4$ T, which is especially important in maintaining $q_{min} > 1$ at low poloidal beta. As beta increases, TRANSP calculations show significant bootstrap current fraction up to 45%, which is believed to cause the observed saturation, or reduction in l_i, and corresponding increase in q_{min}. The importance of increased q_{min} in sustaining stabilization of plasmas above the ideal no-wall beta limit is discussed in Section

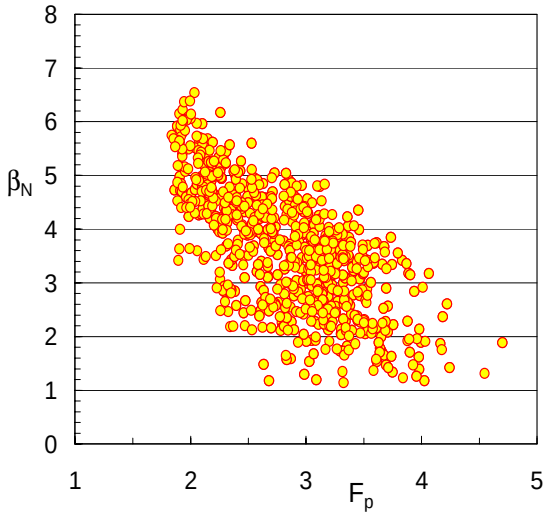

FIG. 2. Normalized beta vs. pressure peaking factor.

3. Beta-limiting MHD instabilities in recent NSTX plasmas are discussed more generally in REF. 5. In this paper, we concentrate on ideal MHD stability limits and the resistive wall mode (RWM). In particular, a comparison is made between RWMs at relatively low β_N and increased static error field and RWM dynamics in high β_N plasmas with reduced error field.

3. Resistive Wall Modes at High Normalized Beta

For a given plasma equilibrium, stable operation at maximum plasma beta theoretically occurs when external kink/ballooning modes are stabilized by a perfectly conducting wall sufficiently close to the plasma boundary (the ideal with-wall beta limit, $\beta_{N\text{wall}}$). However, it has been shown both theoretically [6,7] and experimentally [8,9] that realistic segmented and resistive conducting walls used for actual plasma stabilization allow the destabilization of the resistive wall mode when the plasma beta exceeds $\beta_{N\text{no-wall}}$. The RWM is a plasma mode that is rotating sufficiently slowly ($\Omega \sim 1/\tau_{wall}$) so that the perturbed field can penetrate the wall. Stabilization of the RWM is possible, but requires a rotation rate of order $(k_{||}a)V_A$, where $k_{||}$ is the parallel wave number and V_A is the Alfven speed.[10] This critical rotation frequency, Ω_c, for RWM stabilization has been observed in advanced tokamak experiments [9], and because of the low $k_{||}$ of the mode is a few percent of the Alfven frequency. The RWM typically leads to rotation damping and plasma termination in advanced tokamaks. However, since the mode grows slowly ($\gamma \sim 1/\tau_{wall}$), active feedback stabilization is feasible in plasmas with insufficient toroidal rotation.

While the general concept of the RWM applies to both the advanced tokamak and spherical torus, it is important to study potential differences in the mode physics at low aspect ratio. For example, mode geometry is significantly altered in the ST leading to differences in coupling of the mode to the wall, especially at extremes in β_N. In NSTX, the n = 1 resistive wall mode was initially observed when the ideal no-wall β_N limit was violated in experiments aimed at maximizing coupling of the plasma to the stabilizing conducting plates.[1] The plasmas were limited and did not transition to H-mode. This yielded relatively high F_p = 3.4, and therefore, low $\beta_{N\text{no-wall}} \sim 2.6$, and only a small difference between no-wall and with-wall β_N limits, $\Delta\beta_N = \beta_{N\text{wall}} - \beta_{N\text{no-wall}} = 0.2$. At this low level of β_N, coupling of the mode eigenfunction to the wall can be weak, so the plasma-wall gap was kept small ~ 15% of the plasma minor radius. These experiments were also conducted before the n=1 static error field was reduced. More recently, the RWM has been studied with reduced static error field, in H-mode plasmas with significantly lower $F_p \sim 2$, higher $\beta_N > \beta_{N\text{no-wall}} \sim 4.5$, and larger $\Delta\beta_N = 2$. Primary diagnostics used to detect the mode are an array of saddle coils outside of the vacuum vessel instrumented to measure locked modes, and the plasma toroidal rotation measured by charge exchange recombination spectroscopy. The mode was not observed when $\beta_N < \beta_{N\text{no-wall}}$ as computed by time-evolving ideal MHD stability calculation using DCON.[11] RWMs in plasmas with $\beta_{N\text{no-wall}} \sim 2.6$ either exhibited the RWM or neoclassical tearing modes, but not both. The RWM was observed on the locked mode detector while the plasma stored energy increased. This observation occurred while the plasma was rotating, eliminating the possibility that the mode was a locked tearing mode. No precursors were observed with the magnetic pickup coils, nor were core or edge islands observed before the onset of the RWM. Ultra-soft X-ray emission preceding the beta collapse indicated a kinking of the plasma core. In the comparison plasma, clear n = 2 and n = 3 rotating modes were detected before the beta saturation and ultra-soft X-ray emission showed a radially symmetric reconnection event leading to the termination, rather than a kink. RWMs observed with high static error field generated an n = 1 field perturbation of ~ 7G in the locked mode detector at the time of the beta collapse, that led to plasma termination. The VALEN computed n = 1 mode growth time of 4.6 ms (see Section 4 for detail) agrees well with the experimental RWM growth time of 5 ms from the locked mode detector signal. Based on this calculation, the experimental RWM persisted for $3.5\,\tau_{wall}$ before termination at the beta collapse.

Recent plasmas with reduced static error field and increased β_N exhibit significantly different behavior than RWMs at lower β_N (FIG. 3). First, it is rare to find pure RWM activity separate from tearing mode activity. This observation might be due in part to an increased difficulty in measuring the RWM field perturbation with the present locked mode detector at the reduced static error field. LMD signals of between 0.6 – 1.0 G are now more typical

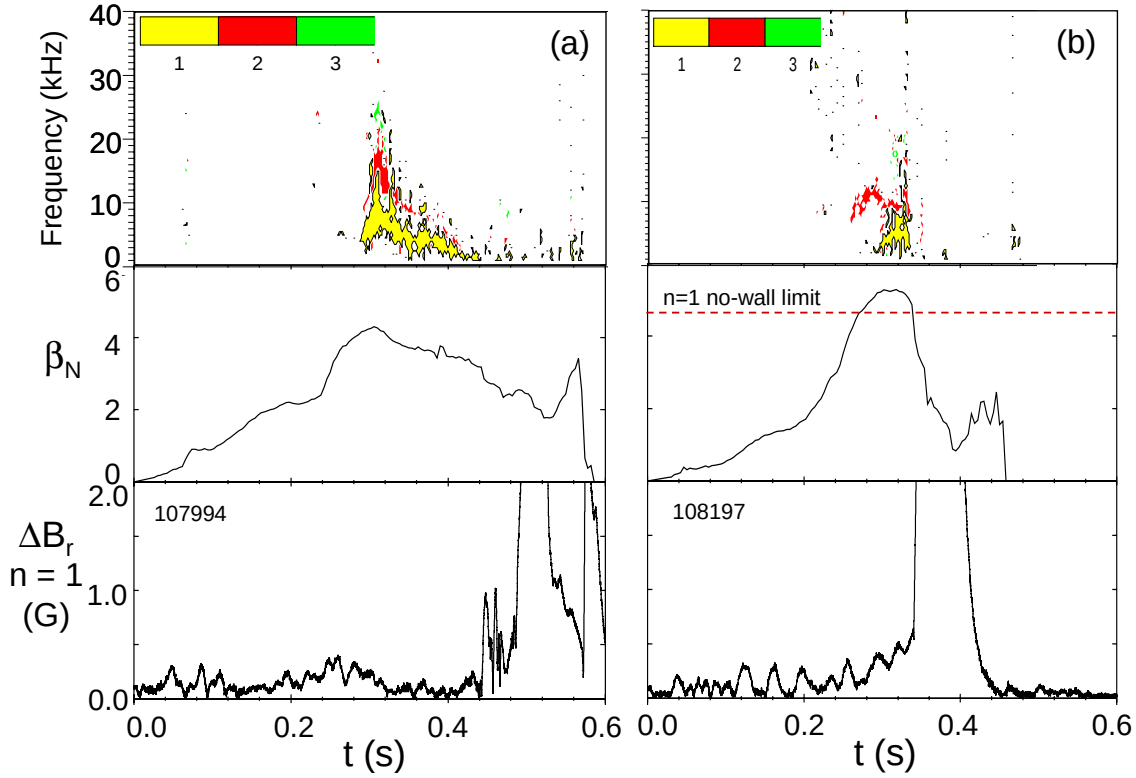

FIG. 3. Time evolution of magnetic pickup coil spectra, β_N, and n=1 locked mode detector signal for a plasma with RWM at high β_N (b) compared to a plasma with no RWM (a).

during the RWM. A common feature between RWMs at high and low β_N is the strong toroidal rotation damping observed in both in spite of increased neutral beam momentum input over lower beta plasmas. The magnitude of the rotation damping, as well as the detail of the rotation profile dynamics distinguishes the RWM from tearing mode activity and suggests a very different physical mechanism for rotation damping between the two modes. In plasmas exhibiting tearing modes, rotation damping is relatively weak. FIG. 4(a) illustrates the toroidal rotation profile dynamics for a plasma initially exhibiting n=1 and 2 rotating mode activity, with n=2 largely damped approximately 60 ms after the mode onset. Magnetic pickup coils show n=1 oscillations with a frequency slowly decreasing from 8 kHz, consistent with the observed toroidal rotation frequency, F_ϕ, decrease in the region of the EFIT computed q=2 surface. The rotation damping rate at q=2 is nearly constant at -29kHz/s. The profile dynamics show the damping to be diffusive, originating near the q=2 surface, and penetrating slowly to the plasma core. Mode locking eventually occurs 0.2s later, when rotation at q=2 drops to the critical value of approximately half the initial value, $\omega_0/2$. This process is in agreement with the theory of rotation damping due to a magnetic island in the presence of a conducting wall. [12] In contrast, FIG. 4(b) shows toroidal rotation damping occurring across most of the plasma cross-section simultaneously when the RWM is present. The process appears non-diffusive, and similar to the rotation damping process observed in error field induced locked modes when field penetration occurs. [13,14] The rotation damping rate near q = 2 in the RWM case is -174 kHz/s, six times more rapid than in the case of islands alone. It is also clear from FIG. 3 that the RWM, that shows only a weak signal in the locked mode detector and is accompanied by n=1 rotating mode activity as the RWM grows. The locked mode detector signal reaches just 0.6 G before the accompanying island locks. The RWM therefore greatly reduces the time it normally takes the island to reach $\omega_0/2$.

Another remarkable detail of the rotation damping process is that the edge rotation remains essentially unchanged during RWM induced rotation damping, whereas the case of slow rotation damping due to islands shows a viscous drag outside of q = 2. This can be qualitatively explained by invoking a model of neoclassical viscous drag[15,16] in the nearly static magnetic field perturbation of the RWM. This model has been successfully used to describe error field induced locked mode damping in JET.[13] By this physics, local rotation

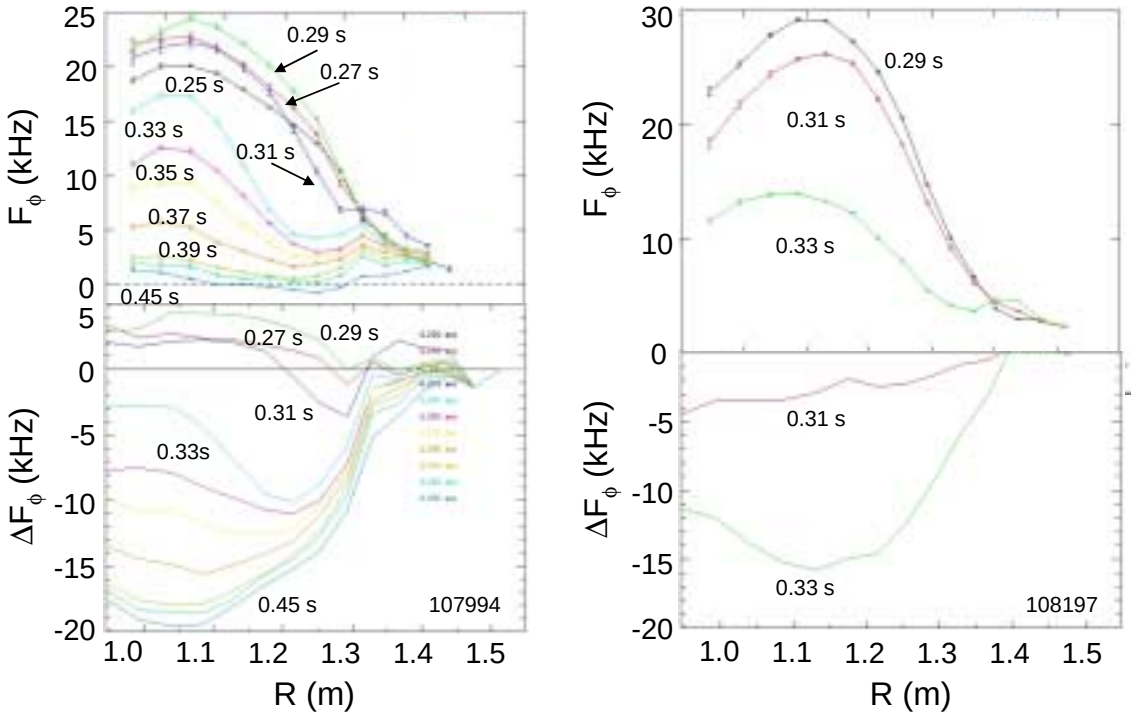

FIG. 4. Toroidal rotation profile dynamics for plasmas with $\beta_N < \beta_{Nno\text{-}wall}$ *exhibiting rotating plasma modes (frame (a)), and* $\beta_N > \beta_{Nno\text{-}wall}$ *exhibiting a resistive wall mode (frame (b)).*

damping scales as $\delta B_r^2 T_i^{0.5}$, where δB_r is the local perturbed field, and T_i is the ion temperature. Therefore, it is expected that the rotation damping would be greatly reduced in the colder outer region of the plasma, consistent with the observation. Profiles of electron temperature from a 20 channel Thomson scattering diagnostic shown in FIG. 5 illustrate the plasma displacement during the growth of the RWM and at constant plasma stored energy. The displacement appears as a global, asymmetric shift of the electron temperature profile. The RWM growth time computed by VALEN is 20 ms, in agreement with the growth rate of the locked mode detector signal.

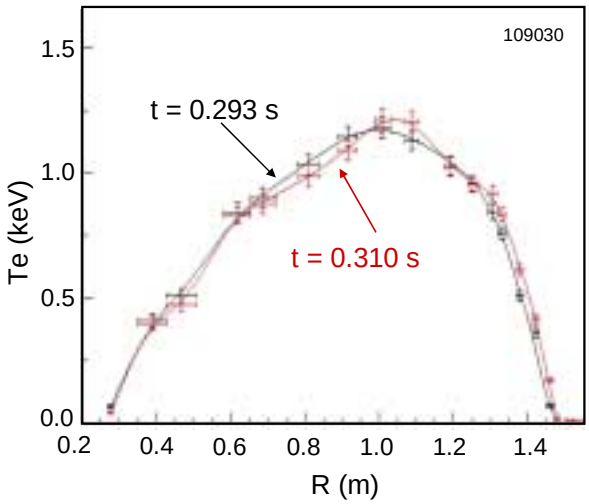

FIG. 5. Electron temperature profile evolution during resistive wall mode growth.

Long pulse ST plasma operation on the order of the global resistive diffusion time with $\beta_N > \beta_{Nno\text{-}wall}$ is a goal of NSTX.[17] Since sufficient plasma rotation is required to stabilize low-*n* kink/ballooning modes, the rapid rotation damping associated with RWM destabilization appears to be a major impediment in reaching this goal. However, present results have already shown significant progress in maintaining $\beta_N > \beta_{Nno\text{-}wall}$ for many resistive wall times. A key to this success has been operation with increased applied toroidal field. FIG. 6 shows the evolution of the toroidal rotation frequency in the core of the plasma for several values of B_0. Also shown is the EFIT computed q_{min} for each plasma at peak β_N. RWMs are observed in the discharges with $B_0 = 0.34$T ($q_{min} = 1.4$) and $B_0 = 0.39$T ($q_{min} = 1.7$), leading to the rapid core rotation damping. However, as B_0 is raised to 0.44T ($q_{min} = 1.9$), the n=1 signature of the RWM is no longer apparent in the locked mode detector signal, the rotation damping rate significantly decreases,

and the pulse length is extended. The fourth case shown also has B_0 = 0.44T, but has slightly different plasma cross-section (increased elongation) and the computed q_{min} rises to slightly above 2. The time-evolution of both β_N and the n=1 ideal MHD stability criteria with and without a conducting wall is shown in FIG. 7 for this discharge. Maximum NBI power (5 MW) is applied at 0.28s (as β_N rises through 4). Although an n=1 perturbation is not observed in the locked mode detector, a slowing of the core toroidal rotation at a rate similar to that experienced during RWM destabilization occurs shortly after β_N increases above $\beta_{Nno\text{-}wall}$ = 4.7 at t=0.296s in this discharge. However during this initial rotation damping stage, q_{min} rises from a minimum value of 1.2 and reaches 2 by 0.32s. From this time until after the first beta collapse at 0.43s, spectra from magnetic pickup coils do not show an n=1 rotating mode in the plasma. Dominant mode activity has n=2 with weaker n=3 present. As β_N continues to rise in the plasma, the core rotation frequency recovers to the original peak value. The VALEN computed RWM growth time when β_N increases beyond $\beta_{Nno\text{-}wall}$ is 15 ms. However, as β_N reaches a peak value of over 6.1, VALEN shows a greatly decreased mode growth time of 30 μs, indicating that β_{Nwall} is being approached and passive wall stabilization has become less effective. At this point, a beta collapse occurs in the plasma reducing β_N to 4.8. The ideal n=1 no-wall stability criterion computed by DCON shows this value to be close to marginal stability. The plasma then recovers and eventually reaches the original peak value of β_N but without an equivalent rise in core rotation frequency. The β_N collapses again back to ideal n=1 no-wall marginal stability, but this time, the toroidal rotation rapidly decreases. During this phase, n=1 locked mode activity is evident but is at the noise level of the detector. A relatively slow decrease in toroidal rotation eventually leads to locking of rotating n=1 and n=2 modes, with a corresponding large collapse in β_N to below $\beta_{Nno\text{-}wall}$. Using the relatively large value of τ_{wall} = 15 ms for the n=1 RWM perturbation computed with DCON and VALEN when β_N initially exceeds $\beta_{Nno\text{-}wall}$, a conservative estimate of the plasma duration with $\beta_N/\beta_{Nno\text{-}wall}$ greater than unity is 18τ_{wall}. The fast, repeated beta collapses shown in FIG. 7 are related to the magnitude of β_N, since similar plasmas have been maintained for longer

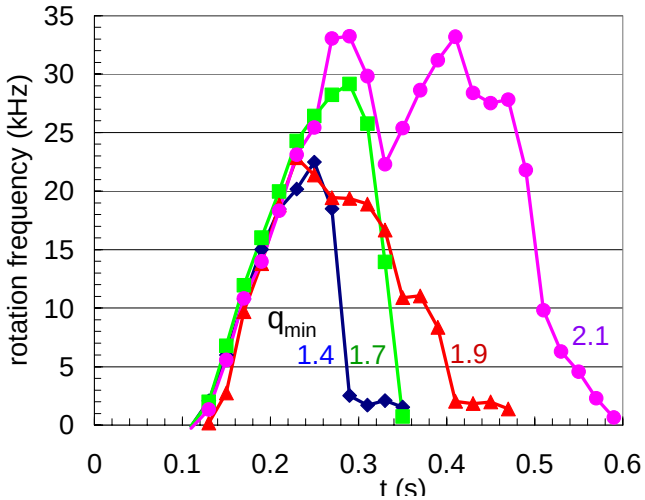

FIG. 6. Variation of toroidal rotation damping dynamics as a function of applied toroidal field (0.34T < B_0 < 0.44T).

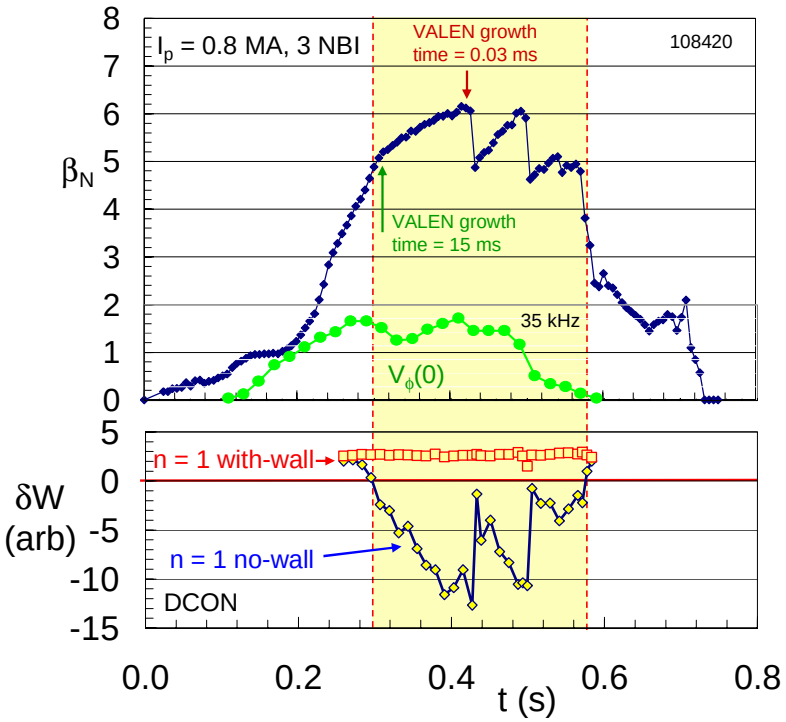

FIG. 7. Evolution of β_N , F_ϕ, and ideal no-wall and with-wall stability criteria for a plasma exceeding $\beta_N/\beta_{Nno\text{-}wall}$=1.3 and approaching β_{Nwall}.

pulse lengths (duration of $25\tau_{wall}$) at a nearly constant value of β_N = 5.6 *without* fast beta collapses. In the discharge shown in FIG. 7, DCON shows that the plasma is also unstable to the n=2 mode shortly after n=1 instability is determined. Plasma instability to multiple n values was anticipated at high β_N, and future work will investigate the presence of n=2 signatures measured by the locked mode detector.

4. Passive Stabilization and Active Feedback Physics Design

Growth rates of resistive wall modes interacting with the complex conducting structures in NSTX device have been computed with the VALEN code.[18] These calculations incorporate the NSTX conducting structure designed to provide passive stabilization of the RWM. VALEN uses a finite element representation of thin shell conducting structures in an integral formulation to model arbitrary conducting walls, combined with a circuit representation of stable and unstable plasma modes. A further capability of VALEN is the ability to model arbitrary control coils, magnetic flux sensors, simple power supplies and control schemes that would be used to connect these items together to provide stabilization of plasma instabilities through active feedback.

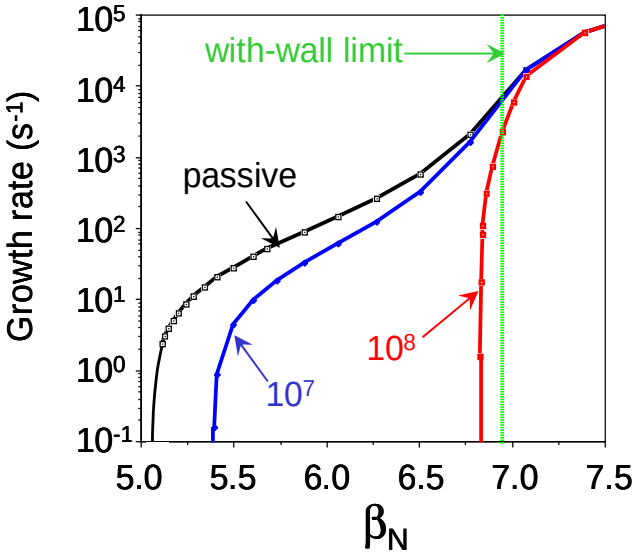

FIG. 8. VALEN growth rate vs. β_N *for the n = 1 mode considering passive, and active feedback systems with gains of* 10^7 *and* 10^8 *V/Wb.*

The external normal field perturbation of the mode to analyze is computed by DCON from reconstructed experimental equilibria. The model of all passive conductors is combined with the unstable plasma mode and VALEN is used to perform an eigenvalue analysis to obtain the growth rate of any instabilities. This procedure may be repeated for different equilibria to obtain a scan in β_N. The eigenvalue from VALEN is the growth rate and the associated eigenvector is the distribution of induced currents in all of the conducting structures. FIG. 8 illustrates the passive growth rates obtained from such a VALEN analysis. For this equilibria scan $\beta_{Nno\text{-}wall}$ is 5.05 and the VALEN estimate of the β_{Nwall} is 6.95. On the right the curve is asymptotic to alfvenic growth rates. The growth rate curves as well as the value of β_{Nwall} depends on the plasma equilibrium parameters. The equilibria used for the scan in FIG. 8 are derived from an NSTX experimental plasma and have F_p ~ 2.2. As in the experiment, for this class of equilibria, we find $\Delta\beta_N$ = 2. Examination of the plasma eigenmode currents shows that along with the greater mode energy at higher β_N, the mode amplitude increases in the divertor region.(FIG. 9) This

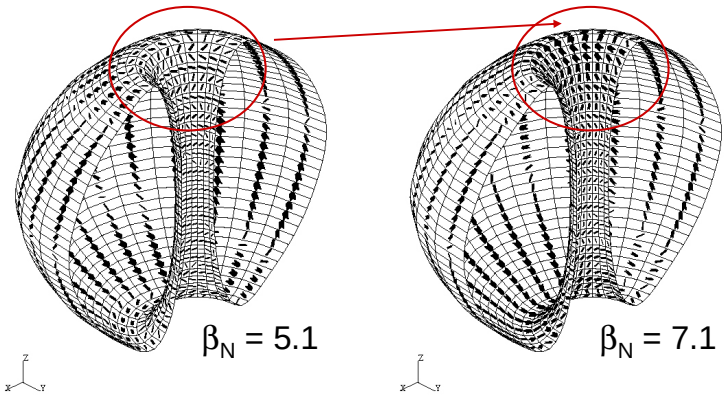

FIG. 9. VALEN computed currents from DCON ideal n=1 external unstable eigenmode. Mode strength increases closer to the divertor region (further from NSTX conducting plates) in high β_N *plasmas.*

migration of the mode away from the conducting plates makes passive stabilization less effective at high β_N. This result is in stark constrast to the behavior of ST plasmas with higher $F_p \sim 3.4$, and lower $\beta_{Nwall} \sim 3$, which have $\Delta\beta_N \sim 0.2$ caused by weak coupling of the RWM in this parameter regime at low aspect ratio. [1].

An active feedback system can be used to stabilize the RWM in a plasma with low toroidal rotation, as is expected in a reactor. Previous calculations using VALEN for the DIII-D device indicate that the most effective systems have control coils positioned as close as possible to the plasma and as far away as possible from major conducting structures. A mode control scheme typically uses a global array of magnetic sensors placed inside the vacuum vessel as close as possible to the plasma and oriented to sample the poloidal field of an instability while being orthogonal to the field produced by the closest control coils. The structure of the instability may then be identified and then feedback logic determines the currents or voltages applied to the control coils.

A near optimal active feedback system designed to suppress the n=1 instability in NSTX has been studied computationally. In this case, the modeled sensors are positioned inside the vacuum vessel on the plasma midplane and measure the poloidal field of the instability. Control coils were placed inside the vacuum vessel. Six equal size picture frame coils, which produce local radial fields, cover the midplane circumference of NSTX and are connected 'anti-pairwise' (control coils diametrically opposite each other are in a series circuit and their radial fields are in the same direction). The sensors have a single turn and an area of 1.e-04 m^2. The flux from the sensors is multiplied by a constant gain to determine the voltage applied to the control coils. A poloidal signature of 1 gauss in a sensor must be multiplied by a gain of 10^8 (V/Wb) to apply one volt to a control coil. FIG. 8 illustrates the performance of this system. At a gain of 10^7 the plasma is stable for beta normal less than 5.39. Further improvement in performance may be obtained by increasing the gain up to about 10^8 where the plasma is stable for beta normal less than 6.83. The active feedback system shows no further improvement for additional increases in gain. Therefore, this system can stabilize the mode in plasmas with β_N up to 94% of the ideal wall limit.

Alternatives to the 'near optimal' active feedback design were considered. The first keeps the poloidal field sensors interior to the vacuum vessel, but moves the control coils outside. This system reaches a maximum stabilized $\beta_N = 0.72\ \beta_{Nwall}$, a decrease of 22% from the near optimal design. The final configuration considered moved the control coils off the midplane and placed them in the gaps between the primary passive plates. The six coils on the midplane are replaced by six coils among the upper primary passive plates and six coils among the lower primary passive plates. The coils no longer produce pure radial field because they have a tilt that matches the primary passive plates. This system reaches only 50% of β_{Nwall}.

---

*Supported by US DOE Contracts DE-FG02-99ER54524 and DE-AC0276CH03073.

[1] SABBAGH, S.A., BELL, R.E., BELL, M.G., et al., Phys. Plasmas **9** (2002) 2085.
[2] HOWL, W., TURNBULL, A.D., TAYLOR, T.S., et al. Phys. Fluids B **4** (1992) 1724.
[3] LAO., L., et al., Nucl. Fusion, **25** (1985) 1611.
[4] MAINGI, R., BELL, M.G., BELL, R.E., et al., Phys. Rev. Lett. **88** (21 Jan 2002) 035003.
[5] MENARD, J.E., BELL, M.G., BELL, R.E., et al., Paper EX/S1-5, this conference.
[6] BONDESON, A., and WARD, D. J., Phys. Rev. Lett. **72** (1994) 2709.
[7] BETTI, R., Phys. Plasmas **5** (1998) 3615.
[8] STRAIT, E.J., TAYLOR, T.S., TURNBULL, A.D., et al., Phys. Rev. Lett. **74** (1994) 2483.
[9] GAROFALO, A.M., STRAIT, E.J., BIALEK, J.M., et al., Nucl. Fusion **40** (2000) 1491.
[10] BETTI, R., and FRIEDBERG, J.P., Phys. Rev. Lett. **74** (1995) 2949.
[11] GLASSER, A.H., and CHANCE, M.S., Bull Am. Phys. Soc. **42** (1997) 1848.
[12] FITZPATRICK, R., Nucl. Fusion, 7 (1993) 1049.
[13] LAZARRO, E., BUTTERY, R.J., HENDER, T.C., et al., Phys. Plasmas **9** (2002) 3906.
[14] LAHAYE, R., GUNTER, S., HUMPHREYS, D.A., et al., Phys. Plasmas **9** (2002) 2051.
[15] SMOLYAKOV, A.I., HIROSE, A., LAZARRO, et al., Phys. Plasmas **2** (1995) 1581.
[16] SHAING, K.C., HIRSHMAN, S.P., CALLEN, J.D., Phys. Fluids **29** (1986) 521.
[17] SYNAKOWSKI, E., BELL, M.G., BELL, R.E., et al., Paper OV/2-2, this conference.
[18] BIALEK, J., BOOZER, A.H., MAUEL, M.E., and NAVRATIL, G.A., Phys. Plasmas **8** (2001) 2170.